Chemical Mapping of Supramolecular Self-Assembled Monolayers via AFM-IR with a Nanometer-Scale Lateral Resolution

Alexandre Dazzi,*,[1] Frank Palmino,[2] Ariane Deniset-Besseau,[1] Jérémie Mathurin,[1] Vincent Luzet,[2] Peter De Wolf,[3] Qichi Hu,[3] Chunzeng Li,[3] Cassandra Philips,[3] and Frédéric Chérioux*,[2]

[1] Université Paris-Saclay, Institut de Chimie-Physique, F-91400 Orsay, France. [2] Université de Franche-Comté, FEMTO-ST, CNRS, F-25000 Besançon, France. [3] Bruker Nano Surfaces, Santa Barbara, CA 93117, USA.

Corresponding Authors

Email: alexandre.dazzi@universite-paris-saclay.fr

Email: frederic.cherioux@femto-st.fr

Supporting Information Placeholder

ABSTRACT: Atomic force microscopy-based photothermal infrared (AFM-IR) techniques have long enabled chemical imaging of surfaces with spatial resolutions down to 10 nanometers. In this study, we push the boundaries of AFM-IR spatial resolution to the single-nanometer scale, achieving chemical mapping of supramolecular networks at the submolecular level. This breakthrough is made possible by implementing an innovative tapping-mode AFM-IR approach. Such unprecedented resolution opens new horizons for advancements in nanoscience

The properties of materials are determined by the composition and arrangement of their components at a nanoscopic level. In numerous fields within nanoscience and nanotechnology, analyzing the chemical compositions, and geometric shapes with spatial resolutions of one nanometer is a fundamental aspect.[1,2] A nondestructive, ambient-compatible, reproducible and reliable method that offers chemically-sensitive imaging along with topographic properties at a spatial resolution of approximately 1 nm, is highly sought after by the research community. Such combined characterization capabilities would undoubtedly expedite progress across a wide array of scientific disciplines. To reach this key-challenge, the combination of atomic force microscopy (AFM) with infrared illumination provides ways to beat the diffraction limit at mid-infrared frequencies.[3,4] During the past decade, peak force infrared microscopy[5] and resonance enhanced force volume IR[6] have been strongly developed. These two techniques are now able to provide nanoscale chemical imaging with a lateral resolution of around ten nanometers.[8-11] Despite these significant advances, current results are mainly limited to the recognition of a nano-object defined by its morphology in standard topography and its infrared signature. This combination has allowed researchers to distinguish between nanoparticles[12] or proteins[13] among other undefined objects, even when the corresponding topographies were not sufficient for differentiation. Although current techniques can now produce topographic images with nanometer-scale contrast differences,[14-16] the analysis of these topographies does not always allow for the determination of the corresponding structural model. This limitation arises because attributing the observed contrast is not always possible, necessitating the use of complementary techniques, such as ultra-high vacuum[15] or solid-liquid scanning tunneling microscopy,[17] to fully establish the models. However, these approaches have the major drawback of requiring additional manipulations (e.g., sample transfer, surface preparation, or re-alignment) which can lead to changes in the acquisition area. Therefore, achieving infrared mapping with resolutions comparable to topographic images has become a crucial objective. This would enable the determination of structural models without manipulating the samples or changing the acquisition area between topographic and infrared spectrum measurements. To achieve this ambitious objective, we implemented an approach to tapping mode AFM-IR by integrating a dual phase-locked loop (PLL) to correct for mode variations. These adjustments enabled us to achieve a lateral resolution of 2.8 nm and a sensitivity of approximately 3 molecules per nm^2 in AFM-IR mapping image. Such precision finally allows for the reliable assignment of contrasts observed in topographical images of a supramolecular monolayer.

The use of Highly Oriented Pyrolytic Graphite (HOPG) as a stable crystalline conductive surface model for the formation of extended 2D supramolecular networks has already been established.[17] Our molecular design features two key components: (i) a carbonyl functional group that acts as an IR marker, and (ii) C18 alkyl chains that promote the formation of extended 2D supramolecular networks on an HOPG surface. This process is driven by a delicate balance between molecule-surface and molecule-molecule interactions.[17] We synthesized an ester derivative (octadecyl 4'-octadecyloxy-4-biphenylcarboxylate, EsterOC18, Figure 1a), based on a biphenyl core flanked by two *n*-octadecyl chains, with one attached to the aromatic core via an ester linkage. The side chain length of the EsterOC18 molecule is 5.27 nm (Figure 1a).

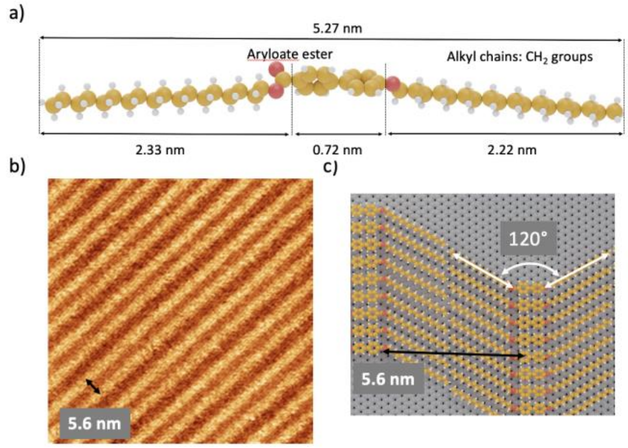

Figure 1. (a) Structural model of octadecyl 4'-octadecyloxy-4-biphenylcarboxyolate (EsterOC18), Oxygen atoms: red, Carbon Atoms; yellow, Hydrogen atoms: grey. (b) Topography AFM image (70×70 nm^2) showing a compact periodic network constituted by bright lines separated by darker stripes with a periodicity of 5.6±0.3 nm, highlighted by the black double arrows. (c) Top view of the proposed molecular model for a monolayer of EsterOC18 on a HOPG surface. the periodicity is shown by the black double arrows.

A sample was prepared by depositing a solution of EsterOC18 molecules (Dichloromethane, $1{\cdot}10^{-5}$ mol·L^{-1}) on an HOPG surface using spin-coating (see method for details). AFM (with Peakforce Tapping Mode using a super sharp probe - SSB - tip) under ambient conditions revealed compact 2D domains. These domains display well-organized bright and dark stripes, with a constant periodicity of 5.6 ± 0.3 nm (Figure 1b). The thickness of these 2D domains was measured at 0.8 ± 0.05 nm on a HOPG surface coated with a sub-monolayer of EsterOC18 molecules (Figure S1). On the basis of these AFM images and our previous results on scanning tunneling microscopy images,[14] we are able to determine the adsorption model describing the 2D monolayers (Figure 1c). We conclude that EsterOC18 molecules align along the <100> direction of the HOPG surface, forming a densely packed 2D layer of parallel, straight *n*-octadecyl chains, consistent with the Groszek model[18] and without interlocking between neighboring chains. However, the contrasts observed in the topography AFM images cannot be definitively attributed to either the aromatic core or the lateral alkyl chains of the EsterOC18 molecule.

The principle of tapping-mode AFM-IR involves driving one cantilever free-air eigenmode to acquire the topography image while using another tapping eigenmode to generate the IR image.[19,20] This nonlinear approach requires that the repetition rate of the IR laser matches the frequency difference or sum between the two eigen modes by a heterodyne detection. Since tapping mode is highly sensitive to the tip-surface interaction, the resonant frequencies shift as the tip scans the sample, responding to mechanical changes in the surface properties. Operating at a fixed laser repetition rate without adjustment can therefore lead to erroneous contrast in the IR mapping. To address this, a phase-locked loop (PLL) has been integrated into the system to ensure that the frequency difference between the two eigen modes remains synchronized, even as the mode frequencies shift during scanning. The frequency of the mode used for topography is set before initiating the approach. The phase of the topography mode is known to exhibit shifts in response to variations in height, mechanical properties, or adhesion. This phase information is commonly used in tapping-mode AFM to identify surface inhomogeneities and, in some cases, to determine mechanical contrasts.[21] These phase shifts indicate changes in the resonance peak position of the mode, leading to a mismatch with the laser repetition rate. To maintain accurate IR mapping, it is essential to correct the frequency shift of the topography mode by adjusting the frequency of the piezo driver to keep the phase constant. The AFM-IR system introduces a dual PLL correction mechanism, one for the topography mode and the other for the IR signal, ensuring that mechanical or topographical effects do not introduce spurious contrast in the IR images (see the complete description in the method section of SI).

The IR fingerprint of the 2D monolayer[14] depicted in Figure S2 was then examined using tapping-mode AFM-IR with the dual PLL correction mechanism. Topography, PLL correction, and chemical mapping of the same region were simultaneously acquired (Figures 2 and S3-4 in SI). Chemical maps were recorded at 1460 and 1600 cm^{-1}, as these two wavenumbers correspond to the CH$_2$ scissoring and C=C stretching vibrations, respectively. These vibrations can unambiguously distinguish the alkyl chains from the aromatic rings of the EsterOC18 molecules. The chemical map recorded at 1740 cm^{-1}, corresponding to C=O bond stretching, is shown in supporting information (Figures S5-6 in SI). Tapping mode AFM topography (Figures 2a-b) and corresponding tracked by PLL frequency image (Figures 2c-d) of a monolayer of EsterOC18 on a HOPG surface display well-organized bright and dark stripes, with a constant periodicity of 5.2 ± 0.3 nm, close to that observed in Figure 1b using AFM Peakforce Tapping Mode (5.6 ± 0.3 nm, Figure 1b). At 1600 cm^{-1}, the signal is extremely weak, and no substructure is observed (Figure 2e). However, unlike our previous work, where the IR mappings showed no substructures at any wavenumber,[15] the images acquired at 1460 cm^{-1} and at 1740 cm^{-1} using the new procedure reveal an alternation of bright and dark stripes (Figures 2f and S5 in SI). To provide a deeper analysis of the chemical mapping recorded at 1460 cm^{-1}, a Z-profile from each AFM image is shown in Figure 2. The signal-to-noise ratio is noticeably higher in the phase images corrected by PLL-frequency (Figures 2d and 2f) compared to the topography image obtained in tapping mode (Figure 2b). In all three cases, the periodicity of the alternating bright and dark stripes is 5.2 ± 0.3 nm. The profiles from both topography and PLL-corrected phase images are in phase, as their maxima and minima align. In contrast, the signal from the IR mapping is out of phase with the other two (Figures 2b, 2d and 2f).

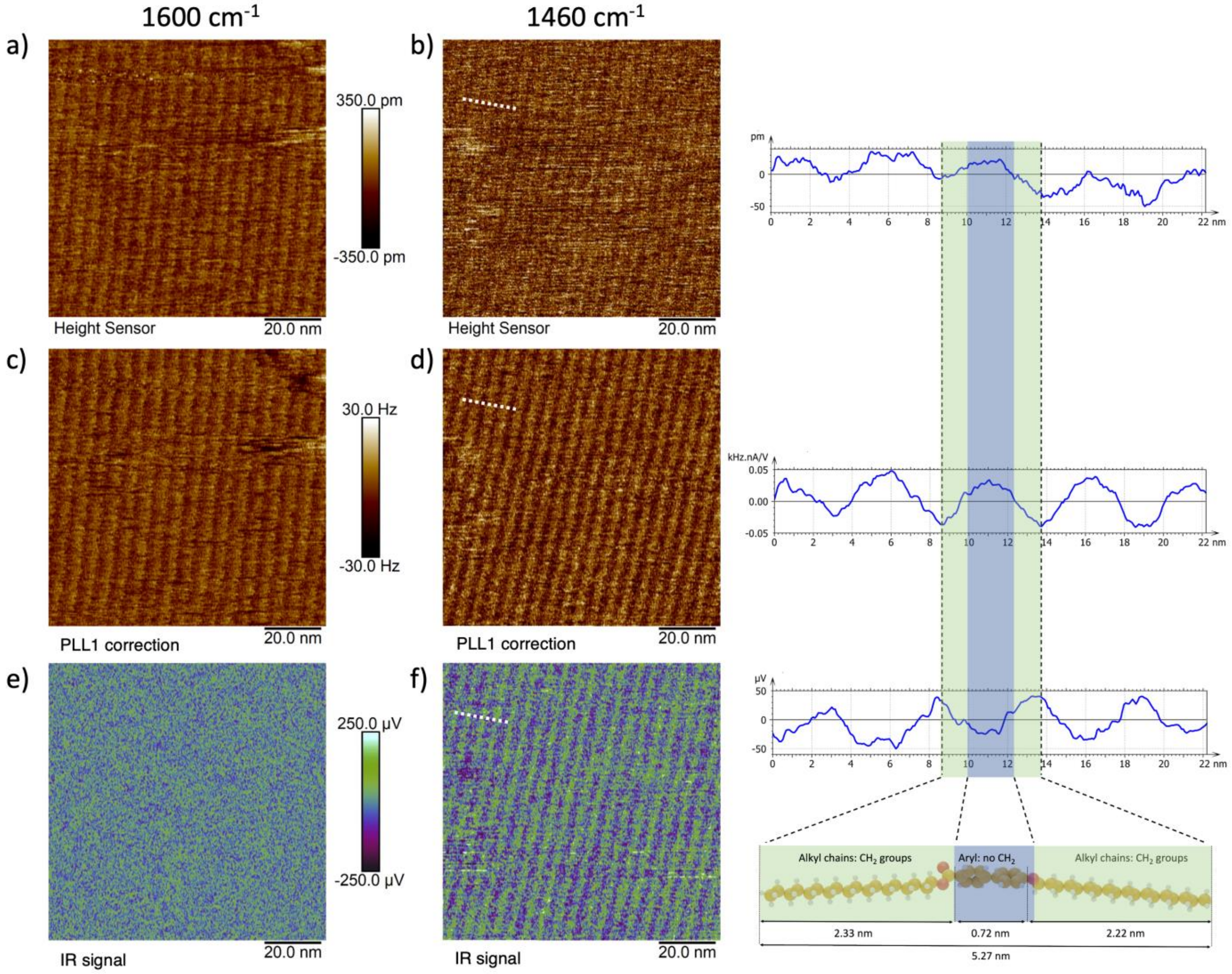

Figure 2. (a) and (b) Topography tapping mode AFM of a monolayer of EsterOC18 on a HOPG surface. (c) and (d) PLL1 correction of the image shown in a) and b) respectively. (e) AFM-IR mapping corresponding to the topography shown in (a) recorded at 1600 cm^{-1} (f) AFM-IR mapping corresponding to the topography shown in (b) recorded at 1460 cm^{-1}. For each image recorded at 1460 cm^{-1}, the corresponding Z-profile taken along the dashed white line is depicted in the right column. The signal corresponding to the alkyl chain is highlighted in green while the absence of signal for the aryl rings is indicated in blue. The scale bar of each image is of 20 nm.

The contrast between the topographic profiles and the infrared mapping has finally enabled an unambiguous assignment of the nature of the light and dark stripes observed in AFM images. Specifically, the dark stripes in the topographic images correspond to the bright stripes at 1460 cm^{-1} in the infrared image, which are characteristic of CH_2 scissoring stretching vibrations. Consequently, the dark stripes in the topography can be attributed to the lateral alkyl chains of the EsterOC18 molecule. Conversely, the bright stripes in the topographic images are attributed to the C=C bonds of these molecules (Figure 2). This finding is remarkable because, until now, the assignment of signals corresponding to subunits within an organic molecule (with dimensions on the order of 5 nm) was achievable through scanning tunneling microscopy or AFM conducted under ultra-high vacuum or by using tip-enhanced Raman spectroscopy.[22]

Based on the chemical mapping recorded at 1740 cm^{-1} (Figure S4 in SI), we estimated the sensitivity of our experimental method. The molecular model of EsterOC18 adsorbed on an HOPG surface is shown in Figure 1c. We calculated the molecular density from this model to be approximately 0.45 molecules per square nanometer. Additionally, we estimated the system's lateral resolution to be 2.8 nm, as the periodicity of the alternating bright and dark stripes is 5.60 ± 0.3 nm (Figure 1b).[23] This suggests that the AFM tip probes a surface area approximately equivalent to a disk of 6.15 nm^2. Since each EsterOC18 molecule contains only one C=O group, we estimated that the sensitivity of AFM-IR mapping in tapping mode corresponds to approximately 2.8 C=O bonds.

Our results represent a significant breakthrough, demonstrating that high-resolution molecular substructure identification can be accomplished using standard AFM techniques coupled with infrared mapping under ambient conditions. This exceptional detection capability of the AFM-IR method paves the way for nanoscale identification of surface-adsorbed molecules or materials even at the single molecule level.

ASSOCIATED CONTENT

Supporting Information.

Detailed description of experimental procedures and additional Z-profiles and AFM images are included in the supporting information.
The Supporting Information is available free of charge on the ACS Publications website.

AUTHOR INFORMATION

Corresponding Author

Email: alexandre.dazzi@universite-paris-saclay.fr
Email: frederic.cherioux@femto-st.fr

Author Contributions

All authors contributed equally.

Funding Sources

No competing financial interests have been declared.

ACKNOWLEDGMENT

The authors acknowledge the financial support from the French National Research Agency through contract ATOMICHEM (ANR-22-CE42-0006) and from the Pays de Montbéliard Agglomération. A.D., A.D.-B., and J.M. acknowledge funding from Paris Ile-de-France Region-DIM "Matériaux anciens et patrimoniaux".

REFERENCES

(1) Barth, J. V.; Constantini, G.; Kern. K. Engineering atomic and molecular nanostructures at surfaces. *Nature* **2005**, *437*, 671-679. DOI: 10.1038/nature04166

(2) Makoudi, Y.; Jeannoutot, J.; Palmino, F.; Chérioux, F.; Copie, G.; Krzeminski, C.; Cleri, F.; Grandidier, B. Supramolecular self-assembly on the B-Si(111)-√3×√3)R30° surface: from single molecules to multicomponent networks. *Surf. Sci. Rep.* **2017**, *72*, 316-349. DOI: 10.1016/j.surfrep.2017.06.001

(3) Dazzi, A.; Prater, C. B. AFM-IR: Technology and applications in nanoscale infrared spectroscopy and chemical imaging. *Chem. Rev.* **2017**, *117*, 5146-5173. DOI: 10.1021/acs.chemrev.6b00448

(4) Mathurin, J.; Deniset-Besseau, A.; Bazin, D.; Dartois, E.; Wagner, M.; Dazzi, A. Photothermal AFM-IR spectroscopy and imaging: Status, challenges and trends. *J. Appl. Phys.* **2022**, *131*, 010901. DOI: 10.1063/5.0063902

(5) Wang, L.; Wang, H.; Wagner, M.; Yan, Y.; Jakob, D. S.; Xu, X. G. Nanoscale simultaneous chemical and mechanical imaging via peak force infrared microscopy, *Sci. Adv.* **2017**, *3*, e1700255. DOI: 10.1126/sciadv.1700255

(6) De Wolf, P. **2024**. Available at https://www.bruker.com/fr/products-and-solutions/infrared-and-raman/nanoscale-infrared-spectrometers/resonance-enhanced-force-volume-refv-afm-ir.html

(7) Dos Santos, A. C. V. D.; Hondl, N.; Ramos-Garcia, V.; Kuligowski, J.; Lendl, B.; Ramer, G. AFM-IR for nanoscale chemical characterization in life sciences: Recent developments and future directions. *ACS Meas. Sci. Au* **2023**, *3*, 301-314, DOI: 10.1021/acsmeasuresciau.3c00010

(8) Xie, Q.; Xu, X. G. What do different modes of AFM-IR mean for measuring soft matter surfaces? *Langmuir*, **2023**, *39*, 17593-17599, DOI: 10.1021/acs.langmuir.3c02950

(9) Nowak, D.; Morrison, W.; Wickramasinghe, H. K.; Jahng, J.; Potma, E.; Wan, L.; Ruiz, R.; Albrecht, T. R.; Schmidt, K.; Frommer, J.; Sanders, D. P.; Park, S. Nanocale chemical imaging by photoinduced force microscopy, *Sci. Adv.* **2016**, *2*, e1501575. DOI: 10.1126/sciadv.1501571

(10) Kurouski, D.; Dazzi, A.; Zenobi, R., Centrone, A. Infrared and Raman chemical imaging and spectroscopy at the nanoscale. *Chem. Soc. Rev.* **2020**, 49, 3315-3347. DOI: 10.1039/C8CS00916C

(11) Centrone, A. Infrared imaging and spectroscopy beyond the diffraction limit. *Ann. Rev. An. Rev.* **2015**, *8*, 101-126. DOI: 10.1146/annurev-anchem-071114-040435

(12) Pancani, E.; Mathurin, J.; Bilent, S.; Bernet-Camard, M.-F.; Dazzi, A.; Deniset-Besseau, A.; Gref, R. High-resolution label-free detection of biocompatible polymeric nanoparticles in cells, *Particle & Particle Systems Characterization* **2018**, *35*, 1700457. DOI:10.1002/ppsc.201700457

(13) Ruggeri, F. S.; Mannini B.; Schmid, R.; Vendruscolo, M.; Knowles, T. P. J. Single molecule secondary structure determination of proteins through infrared absorption nanospectroscopy. *Nature Commun.* **2020**, *11*, 2945. DOI: 10.1038/s41467-020-16728-1

(14) Hamadeh, A.; Palmino, F.; Mathurin, J.; Deniset-Besseau, A.; Grosnit, L.; Luzet, V.; Jeannoutot, J.; Dazzi, A.; Chérioux, F. Toward conformational identification of molecules in 2D and 3D on surfaces, *Commun. Chem.* **2023**, *6*, *246*, DOI: 10.1038/s42004-023-01036-8

(15) Hourani, W.; Lamare, S.; Makoudi, Y.; Palmino, F.; Chérioux, F. Extended monolayer of cyano-ended oligo(para-phenylenes) at the air/HOPG interface investigated by high-resolution AFM. *Nanotechnology* **2016**, *27*, 425601. DOI: 10.1088/0957-4484/27/42/425601

(16) Korolkov, V. V.; Summerfield, A.; Murphy, A.; Amabilino, D. B.; Watanabe, K.; Taniguchi, T.; Beton, P. H. Ultra-high resolution imaging of thin films and single strands of polythiophene using atomic force microscopy. *Nature Commun.* **2019**, *10*, 1537. DOI: 10.1038/s41467-019-09571-6

(17) De Feyter, S.; De Schryver, F. C. Two-dimensional supramolecular self-assembly probed by scanning tunneling microscopy. *Chem. Soc. Rev.* **2003**, *32*, 139-150. DOI: 10.1039/B206566P

(18) Groszek, A. J. Selective adsorption at graphite/hydrocarbon interfaces. *Proc. R. Soc. London Ser. A* **1970**, *314*, 473–498. DOI: 10.1098/rspa.1970.0019

(19) Mathurin, J.; Pancani, E.; Deniset-Besseau, A.; Kjoller, K.; Prater, C. B.; Gref, R.; Dazzi, A. How to unravel the chemical structure and component localization of individual drug-loaded polymeric nanoparticles by using tapping AFM-IR. *Analyst* **2018**, *5940*, 010901. DOI: 10.1039/C8AN01239C

(20) Mathurin, J.; Deniset-Besseau, A.; Dazzi, A. Advanced Infrared Nanospectroscopy Using Photothermal Induced Resonance Technique, AFMIR: New Approach Using Tapping

Mode. Acta. Phys. Pol. A 2020, 137, 29. DOI: 10.12693/APhysPolA.137.29

(21) Magonov, S. N.; Elings, V.; Whangbo, M.-H. Phase imaging and stiffness in tapping-mode atomic force microscopy. *Surf. Sci.* **1997**, *375*, L385. DOI: 10.1016/S0039-6028(96)01591-9

(22) Richard-Lacroix, M; Zhang, Y.; Dong, Z.; Deckert, V. Mastering high resolution tip-enhanced Raman spectroscopy: towards a shiftof perception. *Chem. Soc. Rev*. **2017**, *46*, 3922. DOI: 10.1039/C7CS00203C

(23) Zhang, K.; Bai, Y.; Zhang, Z. Compensation method for correcting the topography convolution of the 3D AFM profile image of a diffraction grating. *Machines* **2024**, *12*, 126. DOI: 10.3390/machines12020126

SYNOPSIS TOC